Electron dynamics in semiconductor interferometers for quantum computing

L. Bellentani[1], A. Beggi[1], P. Bordone[1,2], A. Bertoni[2]

[1]Dipartimento FIM, Universitá di Modena e Reggio Emilia, via Campi 213/A 41125 Modena, Italy

[2]CNR-Istituto Nanoscienze, Modena, Italy

Why a quantum computer?

Qubit: Information is encoded in a quantum bit, a linear combination of the classical bits $|0\rangle$ and $|1\rangle$ with normalized weights.

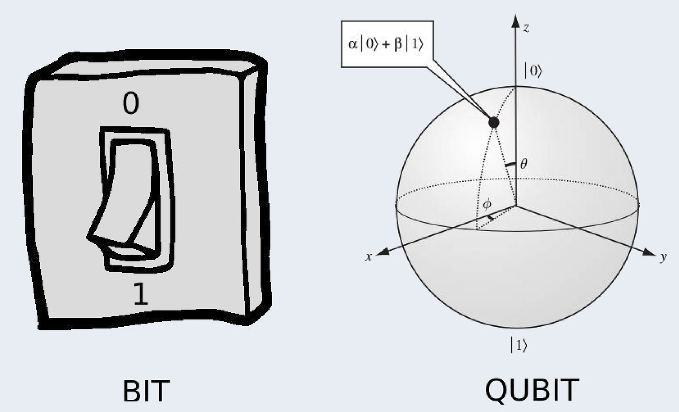

Possible applications:

- **advanced algorithms** to improve computer performances (QFT, quantum search algorithm, quantum oracle);
- possible applications in **quantum information** (quantum teleportation, BB84 protocol)

The main requirements for the implementation of quantum logic gates are **scalability** and **coherence**, which implies the definition of new adequate **nanodevices**.

1.Introduction

- Our system is based on magnetically-driven **edge states** (ESs), which are promising candidates as semiconductor qubits due to their (quasi)immunity to backscattering inside properly designed nanodevices.
- We simulate numerically a **two-channel Mach-Zender interferometer** (MZI), whose geometry guarantees scalability in contrast to the single-channel MZI, previously simulated in Ref.beggi.
- Our software permits to analyze the dynamical properties of electron transport in a time-dependent picture, directly observing the particle dynamics. It requires to describe the travelling carrier as a localized wavepacket (WP), whose time evolution is performed using the **split-step Fourier method**.
- Support calculation with the software Kwant are performed to control the scattering process on the potential landscape. In particolar we focus on the achievement of a beam splitter with 50% interchannel mixing, to guarantee and high visibility of the transmission;
- With a properly design measurement apparatus at the end of the device, we measure the **transmission** of the two-channel MZI and observe Aharonov-Bohm (AB) oscillations.

2.The Mach-Zender interferometer

- At the borders of a laterally-confined **2DEG**, an orthogonal magnetic field **B** generates *edge states*, conductive 1D channels where the electrons can propagate without being backscattered for 'long' distances.
- A properly designed **potential landscape** $V(x,y)$ manipulates such channels, mimicking the effect of the MZI components.

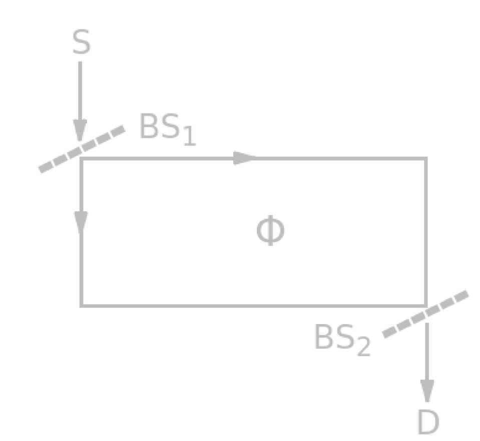

Basics of MZI

- The **shape of the gate components** has an essential role in defining the MZI performances, measured by the visibility of the transmission for the outgoing channel (n=2 in our simulations).

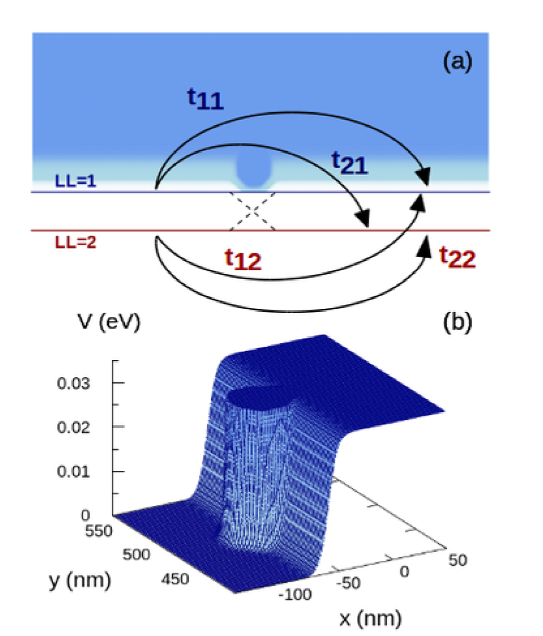

Figure 1: (a) Scattering process at the BS and (b) potential profile adopted for numerical calculations.

The Beam Splitter

The elastic scattering at the BS (Fig.3(b)) redistributes the k components of the wavepacket on the two available channels (Fig.3(a)), generating an essentially 50% inter-channel mixing (Fig.(2)).

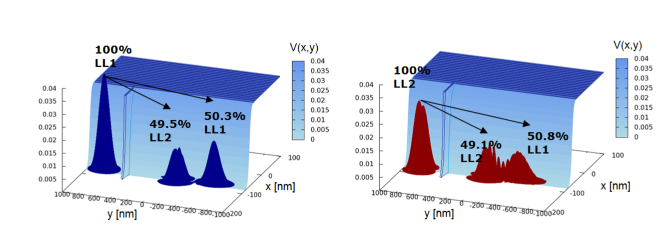

Figure 2: Simulation of the scattering event at the BS for a gaussian WP of ESs initialized in (a)n=1 and (b)n=2.

The Step Potential

A step potential is introduced to separate the two channels. The band for $n=1$ and $n=2$ intersect the energetical bias in two different k, causing a different localization of the two states

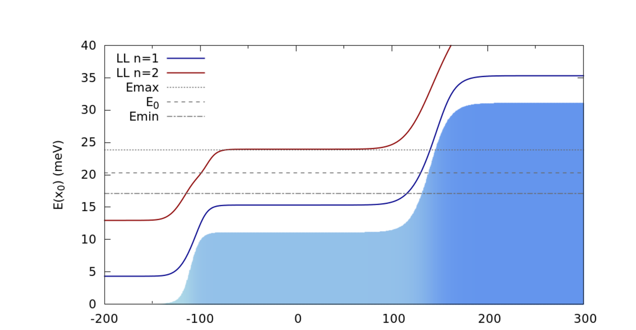

Figure 3: Band structure compared to potential profile along x for the mesa structure

4.Numerical simulations

The initial particle state $\Psi(x,y;0)$ is a **gaussian WP of ESs**, describing a localized charge carrier on the $x-y$ plane. Assuming a non-zero velocity along y, the evolution of the particle state is performed with the **split-step Fourier method**, based on the following equation:

$$\Psi(x,y;t) = e^{\frac{i}{\hbar}\delta t\cdot\frac{\hat{V}}{2}}\left(e^{-\frac{i}{\hbar}\delta t\cdot\hat{V}}\mathcal{F}^{-1}e^{-\frac{i}{\hbar}\delta t\cdot\hat{T}}\mathcal{F}\right)^N e^{-\frac{i}{\hbar}\delta t\cdot\frac{\hat{V}}{2}}\Psi(x,y;0), \quad (1)$$

with $\mathcal{F}$ Fourier-transform operator and $\delta t = 0.1fs$. Eq.1 is implemented in a loop with $N = 4\cdot 10^5$ cycles, where each step i defines the particle state at $t = i\cdot\delta t$.

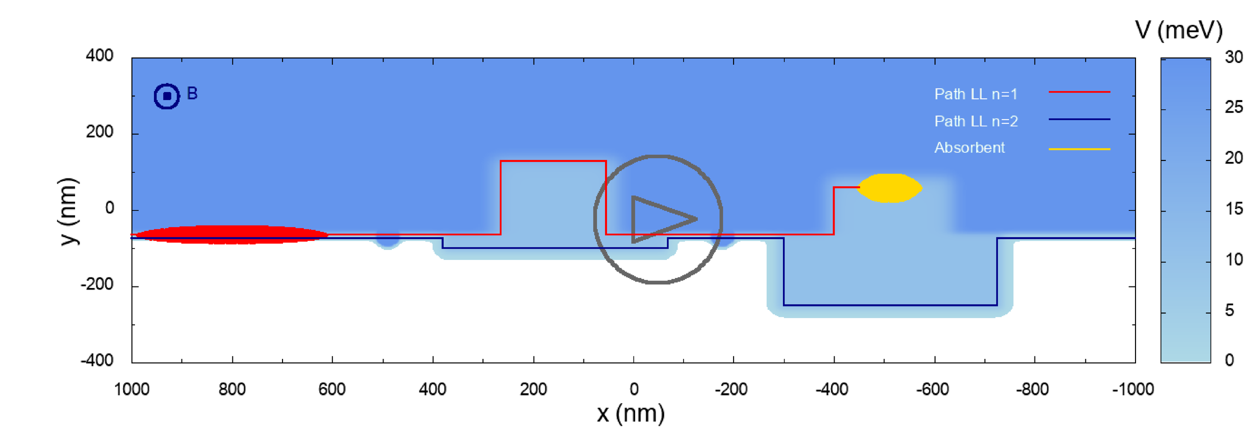

Figure 4: Dynamics of the multichannel MZI for a state initialized in $n=1$, $k_0=-0.3nm^{-1}$ and $\sigma = 60nm$.

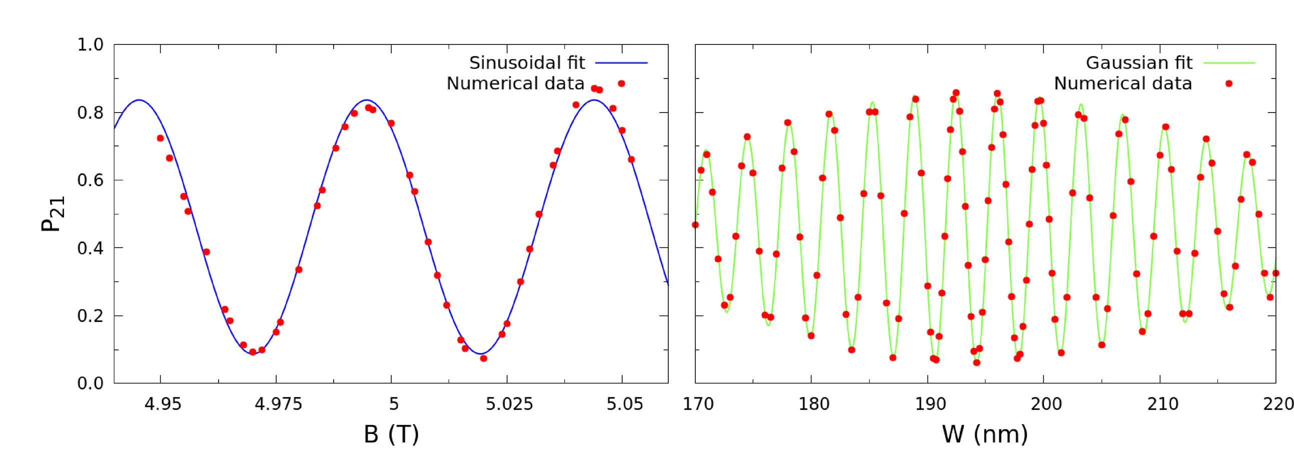

Figure 5: Transmission Probability of the second channel at the end of the multichannel MZI varying (left) the magnetic field B at W=200nm and (right) the width W of the mesa at B=5T. Both plots show AB oscillations and are compared to a simplified analytical model.

- The split-step Fourier method **avoids the computational cost of Hamiltonian diagonalization**, which is required only at $t=0$ in our software;
- Fourier transform requires the Discrete Fourier Transform (DFT) routines in Intel© MKL Library (FFTW interface);
- Runs on Tier-0 **Marconi A1**, Lenovo NextScale supercomputer of CINECA equipped with 2 x 18-cores Intel© Xeon E5-2697 v4 at 2.30 GHz per node (totally 1.512 nodes);
- Parallelization is exploited with the **shared-memory paradigm** in OpenMP on a single MPI proc for the loop based on eq. (1).

6.Discussion and Perspectives

- The optimization of BS performances ensures an **high visibility** in AB oscillations ($\sim 87\%$), which differs to unity due to a slight energy dependence of the scattering process at the BS and mesa and a partial filling of the third Landau level.
- **Damping** of intensity in Fig.5(b) is a unique result of the adopted time-dependent approach and **contains information about carrier localization**. The interference is indeed suppressed when the length mismatch between the two paths approaches to σ.
- Our single-particle simulations validate this system for the implementation of **single-qubit logic gates**. The simulation of two interacting carriers should expose its ability to create two-qubits gates.
- We plan to **include electron-electron interaction** between two copropagating wavepackets, described by an anti-symmetric fermionic state $\Psi(x_1,y_1,x_2,y_2;t)$. The evolution of such state requires the partition of the simulation grid between different MPI processors, to go beyond the present limitation of memory consumption. (GPU?)
- We finally aim to assess the quantum entanglement created between the two carriers exploiting two-particle interference in Hong-ou-Mandel and **Handbury-Brown-Twiss** experiments.

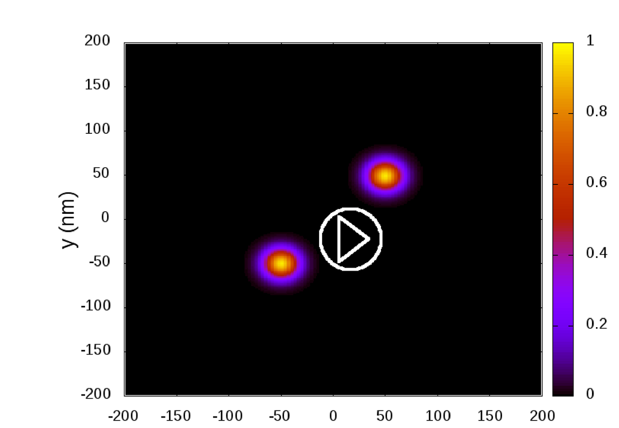

Figure 6: Dynamics of two interacting coherent states -quantum counterparts of the cyclotron orbits- with opposite velocities

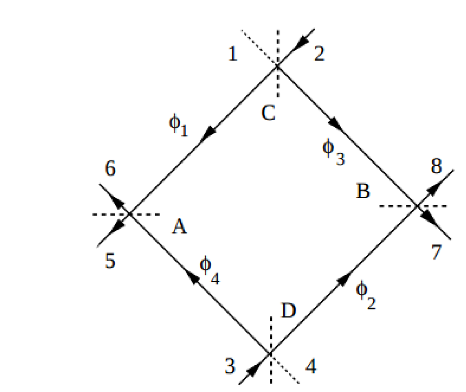

Figure 7: Setup of an optical Handbury-Brown-Twiss interferometer from Ref.[3]

References

[1] A. Beggi et al. *J. Phys.: Cond. Matt.* **27**, 475301 (2015)

[2] V. Giovannetti et al. *Phys Rev B* **77**, 155320 (2008)

[3] P. Samuelsson et al. *Phys Rev Letters* **92**, 026805 (2004)

Electron dynamics in semiconductor interferometers for quantum computing

L. Bellentani[1], A. Beggi[1], P. Bordone[1,2], A. Bertoni[2]

[1]Dipartimento FIM, Universitá di Modena e Reggio Emilia, via Campi 213/A 41125 Modena, Italy

[2]CNR-Istituto Nanoscienze, Modena, Italy

Why a quantum computer?

Qubit: Information is encoded in a quantum bit, a linear combination of the classical bits $|0\rangle$ and $|1\rangle$ with normalized weights.

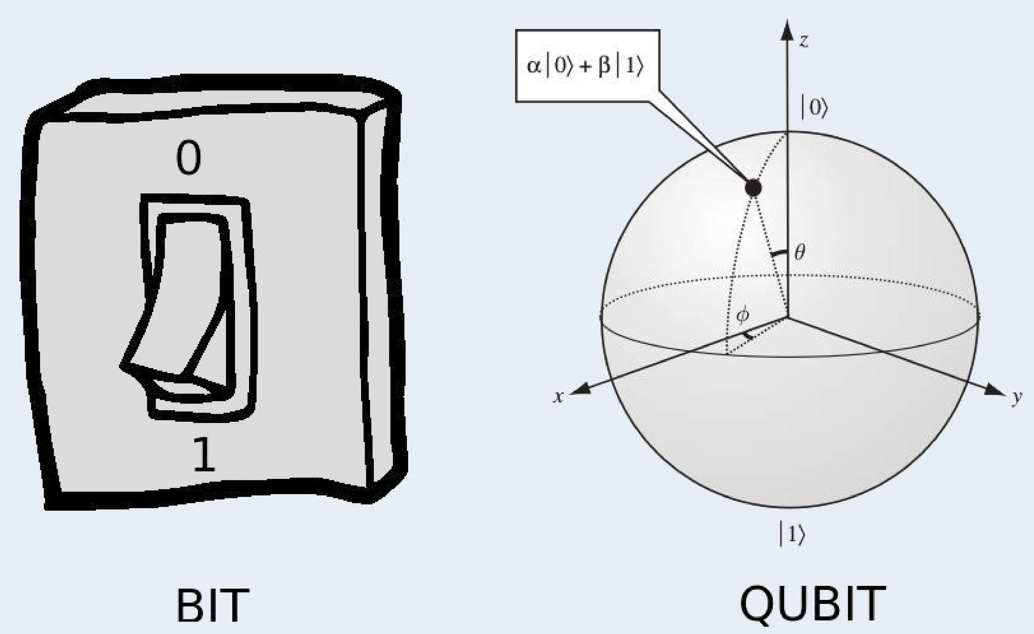

Possible applications:

- **advanced algorithms** to improve computer performances (QFT, quantum search algorithm, quantum oracle);
- possible applications in **quantum information** (quantum teleportation, BB84 protocol)

The main requirements for the implementation of quantum logic gates are **scalability** and **coherence**, which implies the definition of new adequate **nanodevices**.

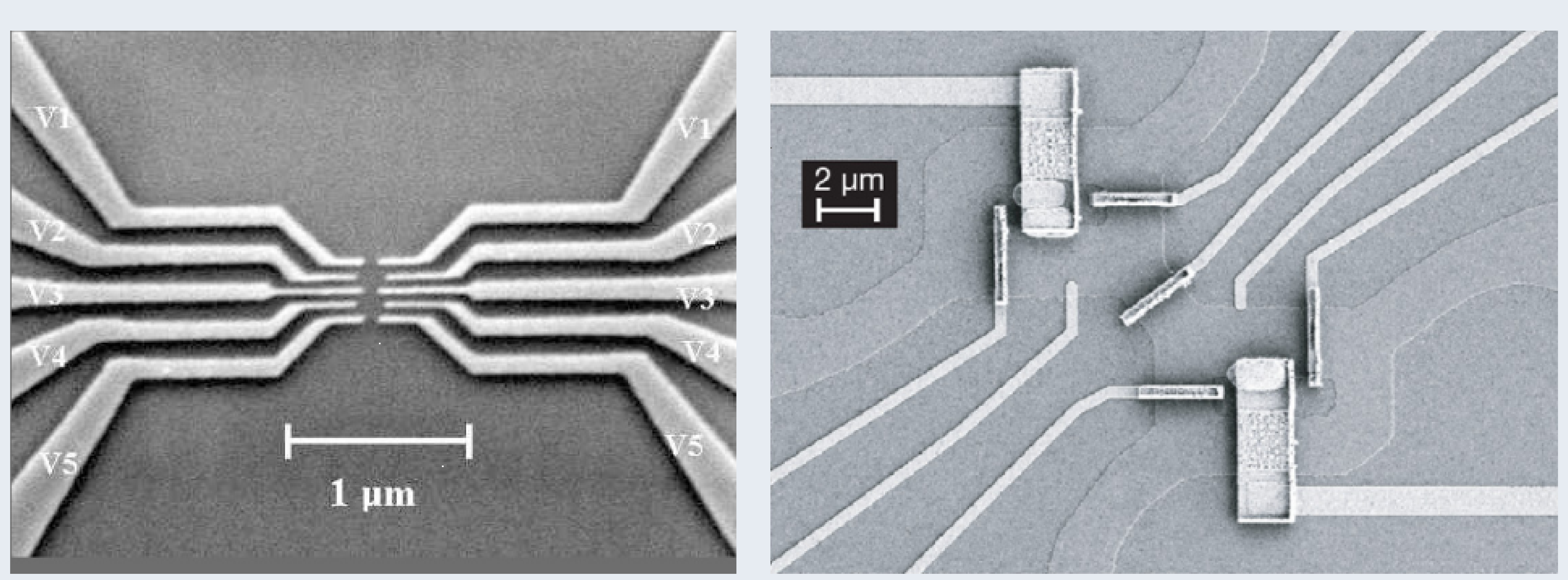

Figure: Examples of nanodevices: (left) Quantum Dot, (right) Handbury-Brown-Twiss interferometer

1.Introduction

- Our system is based on magnetically-driven **edge states** (ESs), which are promising candidates as semiconductor qubits due to their (quasi)immunity to backscattering inside properly designed nanodevices.
- We simulate numerically a **two-channel Mach-Zender interferometer** (MZI), whose geometry guarantees scalability in contrast to the single-channel MZI, previously simulated in Ref[1].
- Our software permits to analyze the dynamical properties of electron transport in a time-dependent picture, directly observing the particle dynamics. It requires to describe the travelling carrier as a localized wavepacket (WP), whose time evolution is performed using the **split-step Fourier method**.

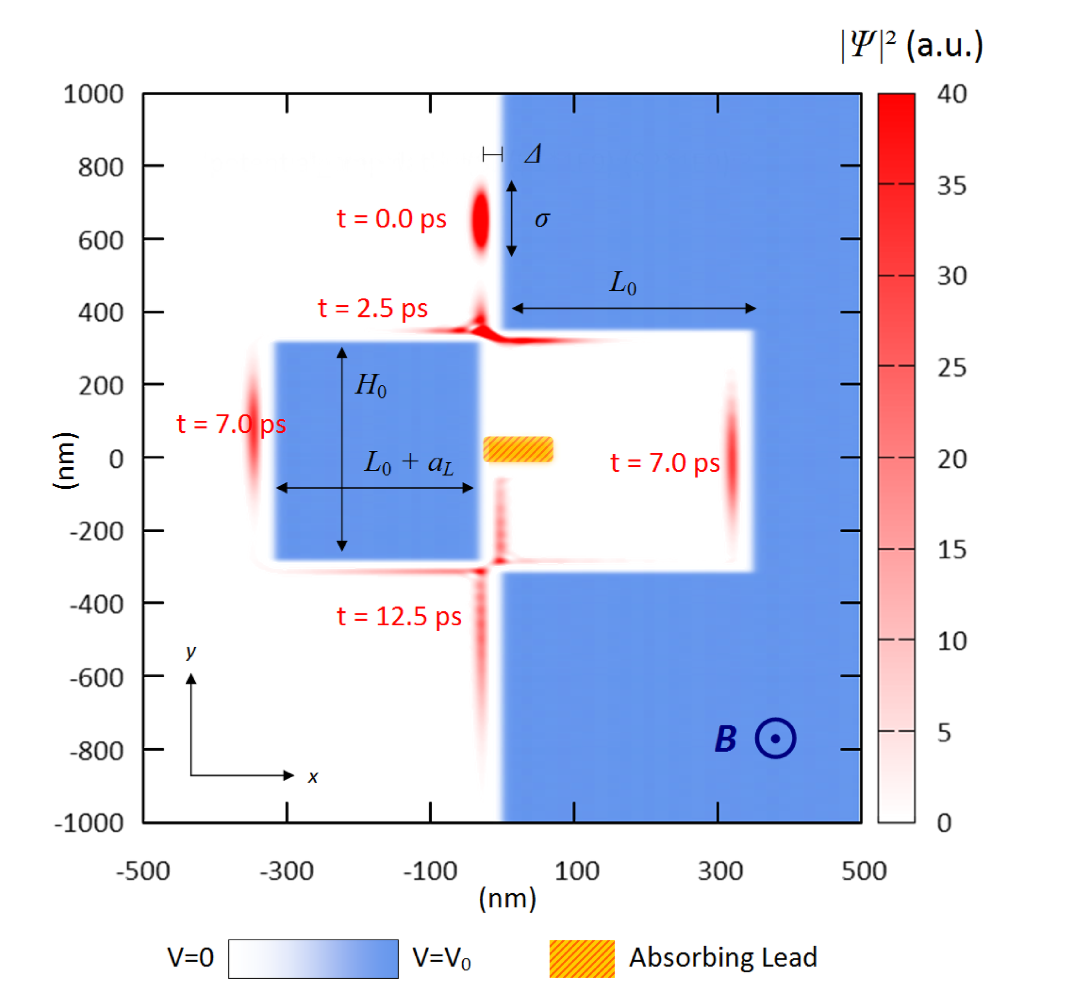

Figure: Geometry adopted for the single-channel MZI in Ref[1].

- Support calculation with the software Kwant are performed to control the scattering process on the potential landscape. In particolar we focus on the achievement of a beam splitter with 50% interchannel mixing, to guarantee and high visibility of the transmission;
- With a properly design measurement apparatus at the end of the device, we measure the **transmission** of the two-channel MZI and observe Aharonov-Bohm (AB) oscillations.

Electron dynamics in semiconductor interferometers for quantum computing

L. Bellentani[1], A. Beggi[1], P. Bordone[1,2], A. Bertoni[2]
[1]Dipartimento FIM, Universitá di Modena e Reggio Emilia, via Campi 213/A 41125 Modena, Italy
[2]CNR-Istituto Nanoscienze, Modena, Italy

3.The Mach-Zender Interferometer

- At the borders of a laterally-confined **2DEG**, an orthogonal magnetic field **B** generates *edge states*, conductive 1D channels where the electrons can propagate without being backscattered for 'long' distances.

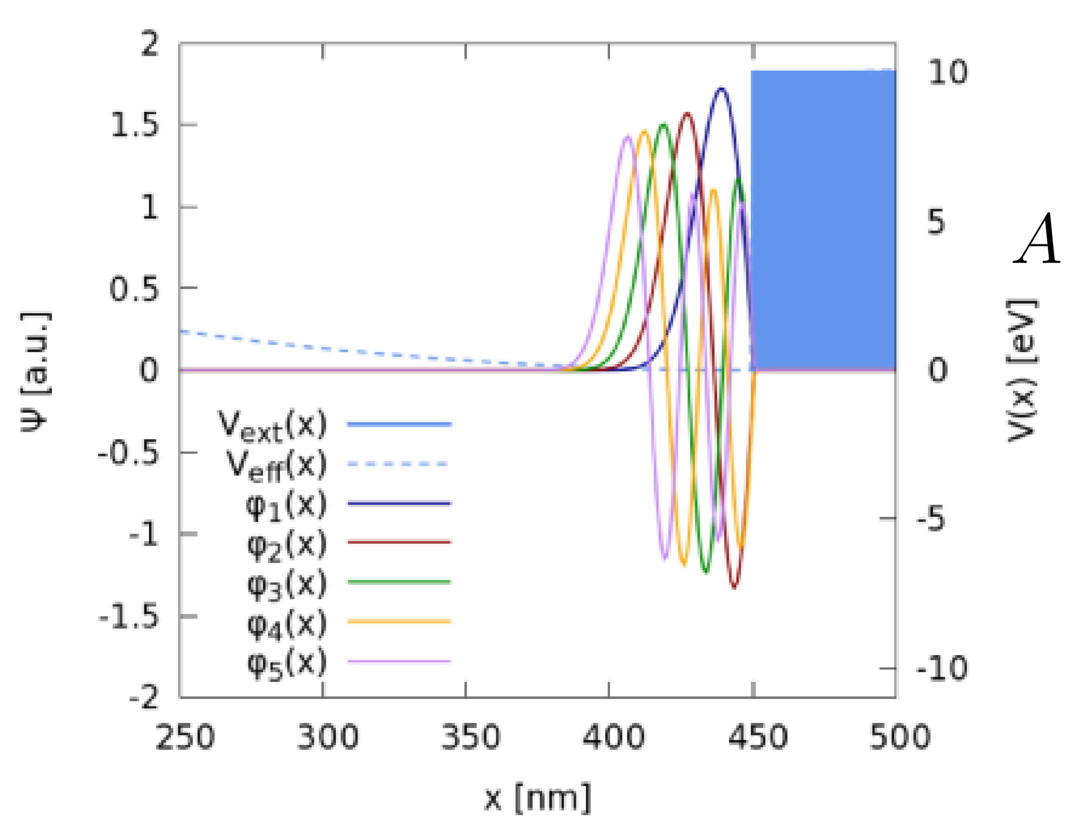

$$\hat{H}(x,y) = \frac{1}{2m^*}(\hat{p} - e\hat{A})^2 + V(x,y)$$

$$A = B(0,x,0) \rightarrow \hat{H}(x,y) = \hat{H}^{1D}_{eff}(x) + \hat{H}(y)$$

$$\Psi(x,y) = \phi_n(x)e^{iky}$$

$$\hat{H}^{1D}_{eff}(x) = \hat{T}(p_x) + \frac{1}{2}m^*\omega_c^2(x - x_0)^2$$

$$x_0 = -\frac{\hbar}{eB}k$$

- A properly designed **potential landscape** $V(x,y)$ manipulates such channels, mimicking the effect of the MZI components.

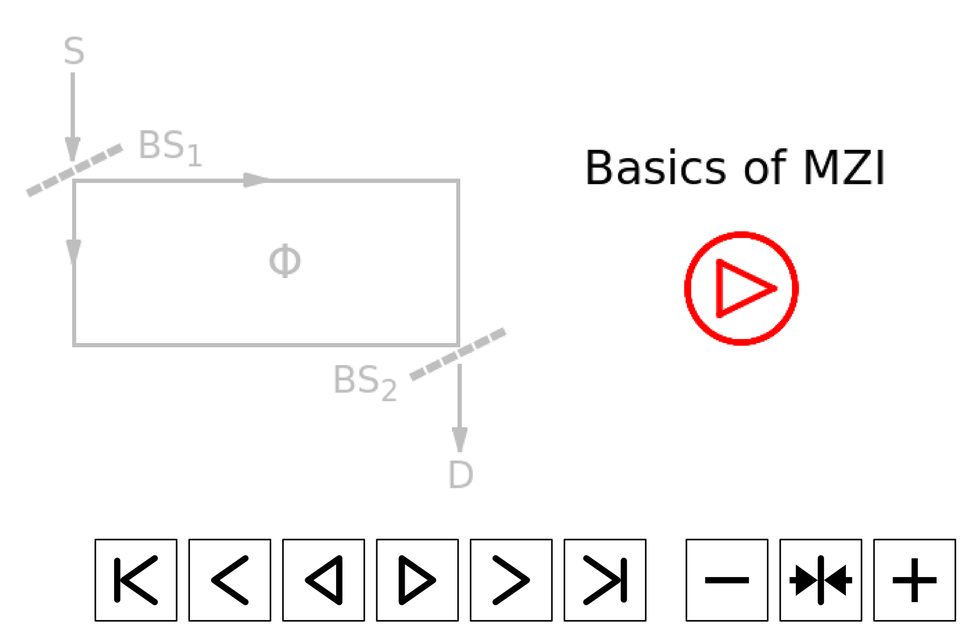

- The **shape of the gate components** has an essential role in defining the MZI performances, measured by the visibility of the transmission for the outgoing channel (n=2 in our simulations).

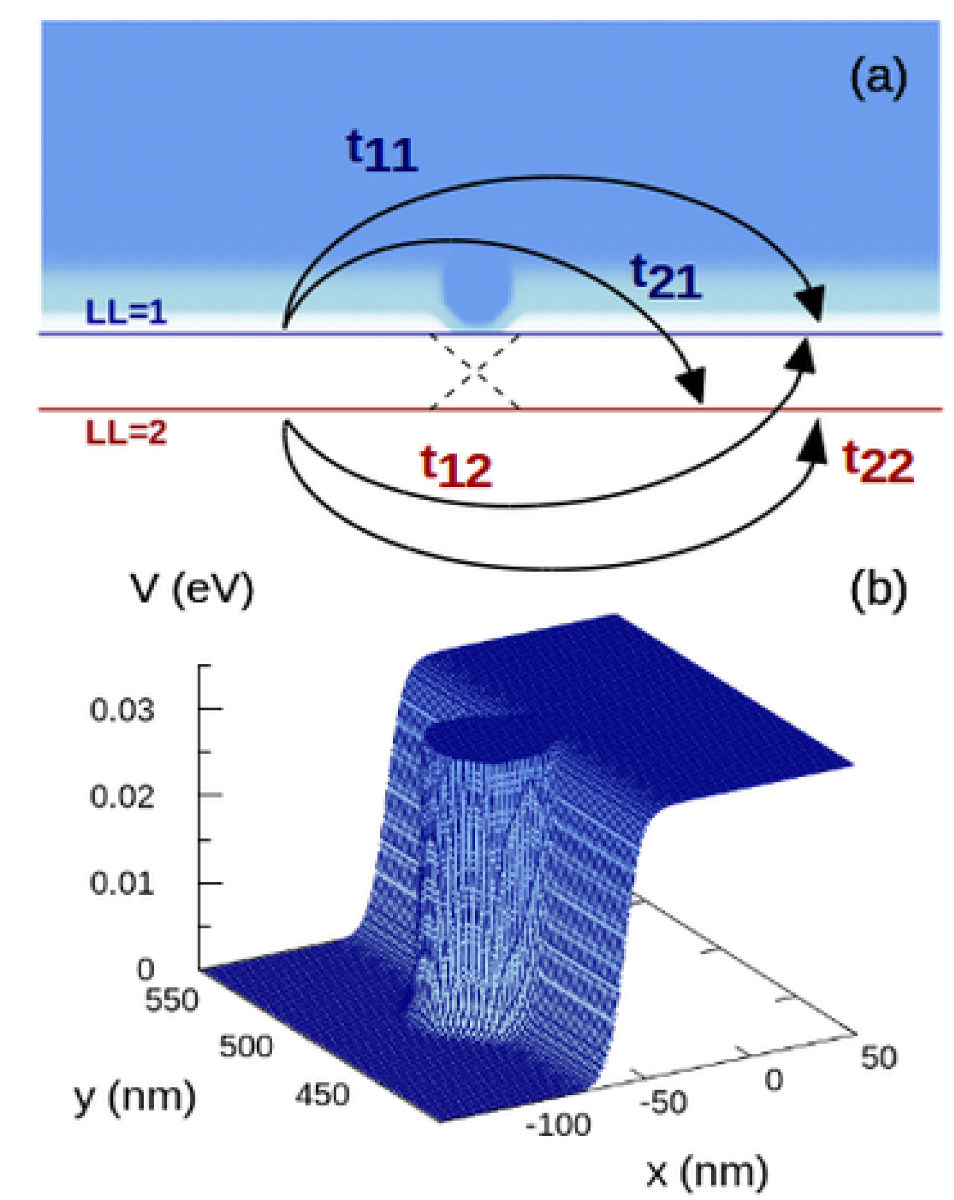

Figure: (a) Scattering process at the BS and (b) potential profile adopted for numerical calculations.

The Step Potential

A step potential is introduced to separate the two channels. The band for $n = 1$ and $n = 2$ intersect the energetical bias in two different k, causing a different localization of the two states. Smoothness is required to avoid additional unwanted mixing.

The Beam Splitter

The elastic scattering at the BS redistributes the k components of the gaussian wavepacket on the two available channels, generating an essentially 50% interchannel mixing. Sharpness and proper tuning of B and E are required.

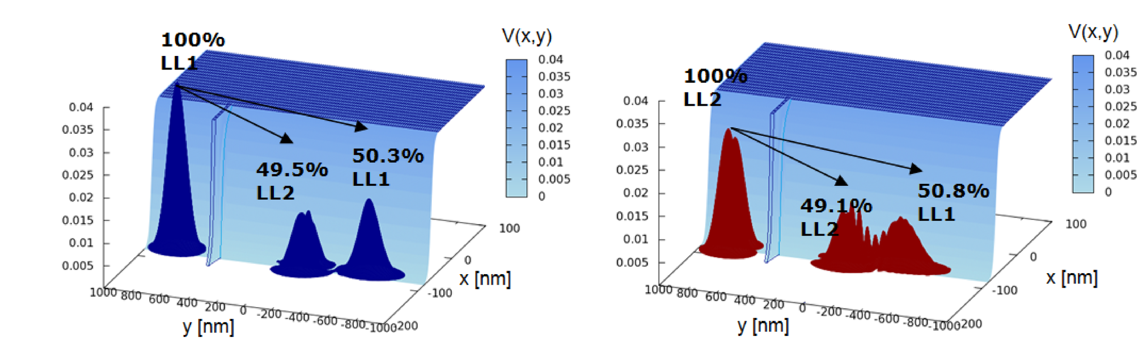

Figure: Simulation of the scattering event at the BS for a gaussian WP of ESs initialized in (a)n=1 and (b)n=2.

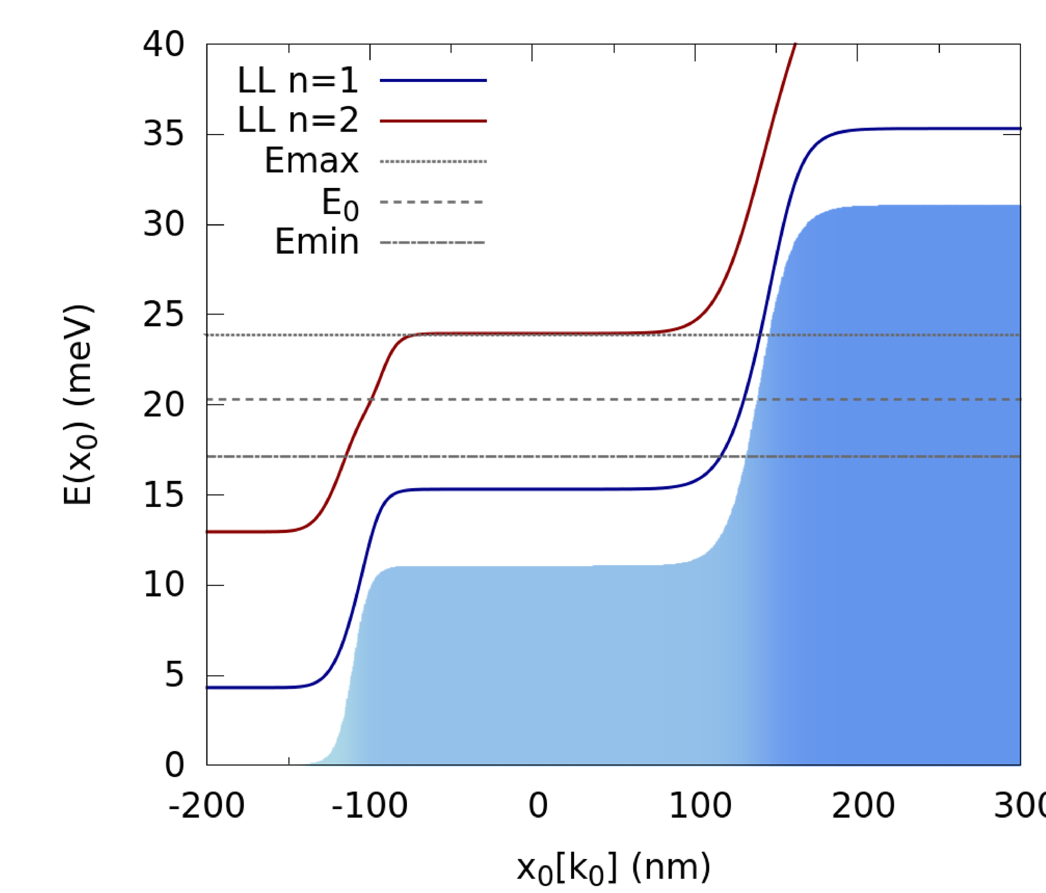

Figure: Band structure compared to potential profile along x for the mesa structure

Electron dynamics in semiconductor interferometers for quantum computing

L. Bellentani[1], A. Beggi[1], P. Bordone[1,2], A. Bertoni[2]
[1]Dipartimento FIM, Universitá di Modena e Reggio Emilia, via Campi 213/A 41125 Modena, Italy
[2]CNR-Istituto Nanoscienze, Modena, Italy

4.Numerical simulations

The initial particle state $\Psi(x, y; 0)$ is a **gaussian WP of ESs**:

$$\Psi_n(x, y; 0) \propto \int dk e^{-\sigma^2(k-k_0)^2} e^{-iky_0} \phi_{n,k}(x) e^{iky}$$

describing a localized charge carrier on the $x-y$ plane. Assuming a non-zero velocity along y, the evolution of the particle state is performed with the **split-step Fourier method**, based on the a clever split of the evolution operator:

$$e^{-i\frac{H}{\hbar}\delta t} \sim e^{-i\frac{T}{\hbar}\delta t} \cdot e^{-i\frac{V}{\hbar}\delta t}$$
$$e^{-i\frac{T}{\hbar}\delta t} \longrightarrow \text{diagonal in k-space} \rightarrow \text{apply } \mathcal{F}$$
$$e^{-i\frac{V}{\hbar}\delta t} \longrightarrow \text{diagonal in r-space} \rightarrow \text{apply } \mathcal{F}^{-1}$$

The final state is:

$$\Psi(x, y; t) = e^{\frac{i}{\hbar}\delta t \cdot \frac{\hat{V}}{2}} (e^{-\frac{i}{\hbar}\delta t \cdot \hat{V}} \mathcal{F}^{-1} e^{-\frac{i}{\hbar}\delta t \cdot \hat{T}} \mathcal{F})^N e^{-\frac{i}{\hbar}\delta t \cdot \frac{\hat{V}}{2}} \Psi(x, y; 0)$$

with $\mathcal{F}$ Fourier-transform operator and $\delta t = 0.1 fs$. The equation is implemented in a loop with $N = 4 \cdot 10^5$ cycles, where each step i defines the particle state at $t = i \cdot \delta t$.

- The split-step Fourier method **avoids the computational cost of Hamiltonian diagonalization**, which is required only at $t = 0$ in our software;
- Fourier transform requires the Discrete Fourier Transform (DFT) routines in Intel© MKL Library (FFTW interface).
- Runs on Tier-0 **Marconi A1**, Lenovo NextScale supercomputer of CINECA equipped with 2 x 18-cores Intel© Xeon E5-2697 v4 at 2.30 GHz per node (totally 1.512 nodes);
- Parallelization is exploited with the **shared-memory paradigm** in OpenMP on a single MPI proc.

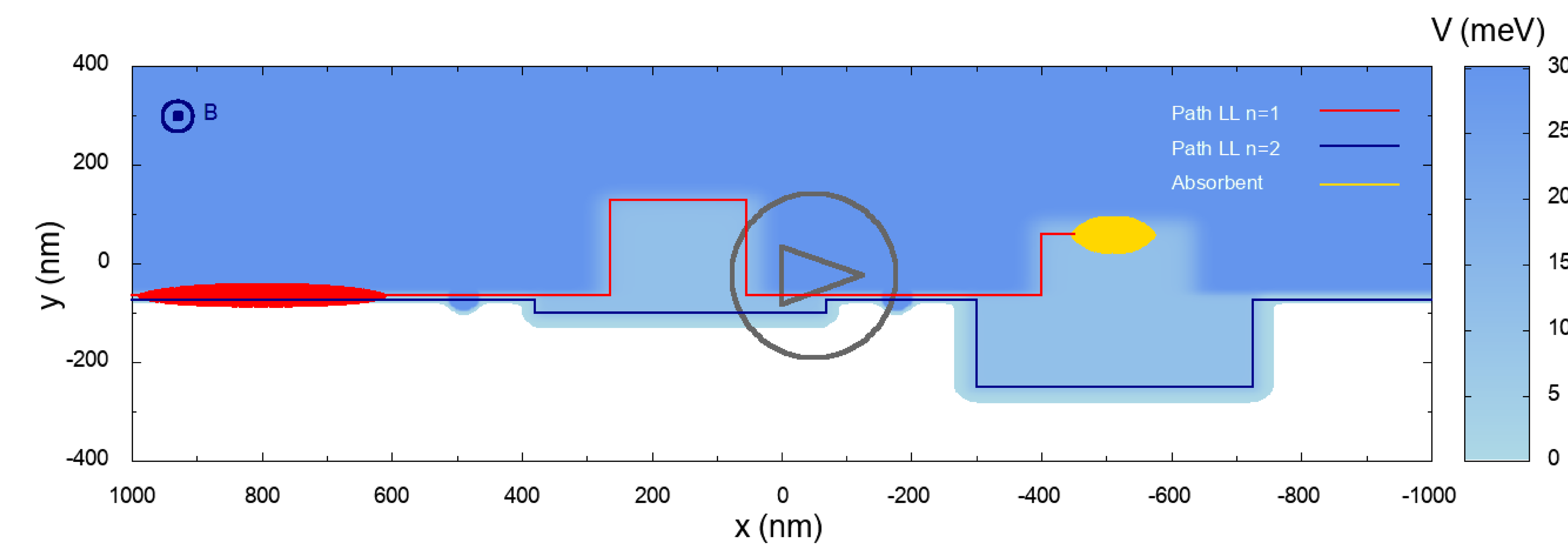

Figure: Dynamics of the multichannel MZI for a state initialized in $n = 1$, $k_0 = -0.3nm^{-1}$ and $\sigma = 60nm$.

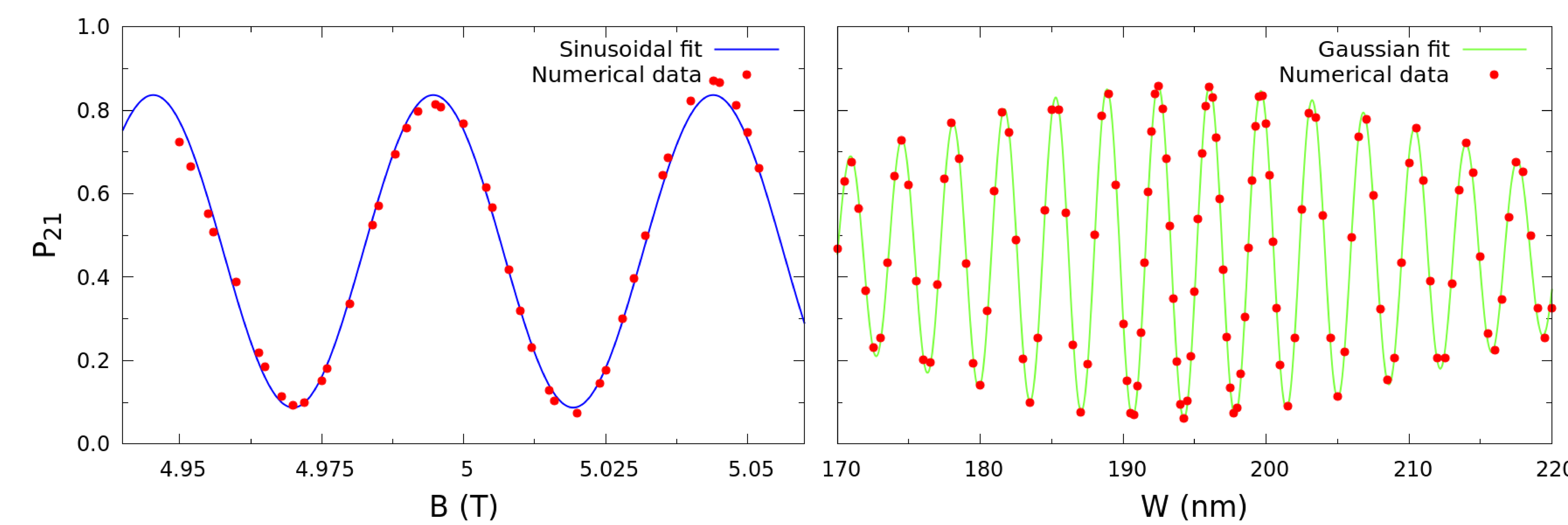

Figure: Transmission Probability of the second channel at the end of the multichannel MZI varying (left) the magnetic field B at W=200nm and (right) the width W of the mesa at B=5T. Both plots show AB oscillations and are compared to a simplified analytical model

Electron dynamics in semiconductor interferometers for quantum computing

L. Bellentani[1], A. Beggi[1], P. Bordone[1,2], A. Bertoni[2]

[1]Dipartimento FIM, Universitá di Modena e Reggio Emilia, via Campi 213/A 41125 Modena, Italy
[2]CNR-Istituto Nanoscienze, Modena, Italy

5.Discussion and Perspectives

- The optimization of BS performances ensures an **high visibility** in AB oscillations ($\sim 87\%$), which differs to unity due to a slight energy dependence of the scattering process at the BS and mesa and a partial filling of the third Landau level.
- **Damping** of intensity in Fig.5(b) is a unique result of the adopted time-dependent approach and **contains information about carrier localization**. The interference is indeed suppressed when the length mismatch between the two paths approaches to σ.
- Our single-particle simulations validate this system for the implementation of **single-qubit logic gates**. The simulation of two interacting carriers should expose its ability to create two-qubits gates.

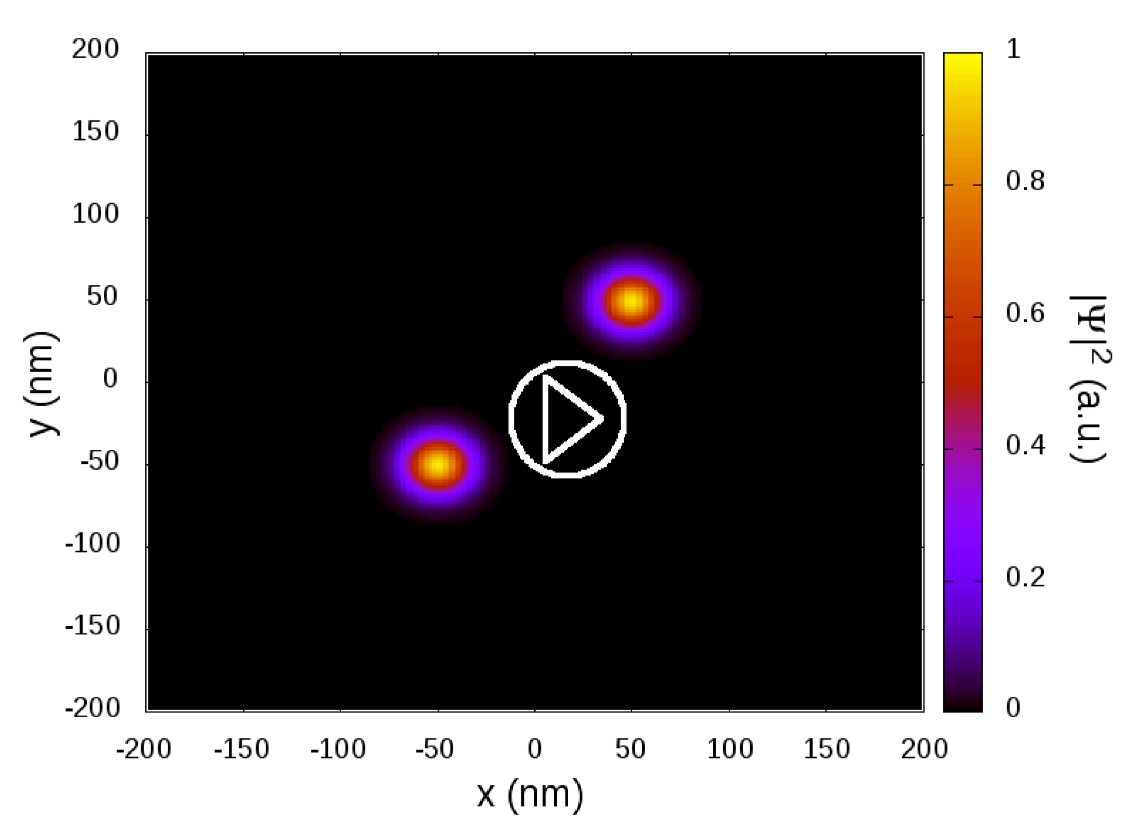

Figure: Dynamics of two interacting coherent states (qunatum counterpart of cyclotron orbits) with opposite velocities. Main limitation is memory consomption.

- We plan to **include electron-electron interaction** between two copropagating wavepackets, described by an antisymmetric fermionic state $\Psi(x_1, y_1, x_2, y_2; t)$. The evolution of such state requires the partition of the simulation grid between different MPI processors, to go beyond the present limitation of memory consumption.
- We finally aim to assess the quantum entanglement created between the two carriers exploiting two-particle interference in Hong-ou-Mandel and **Handbury-Brown-Twiss** experiments.

Appendix

Support calculation are performed with the Kwant software, using delocalized plane waves. The lower computational cost allows to simulate also the injection and collection mechanism (L_1, L_2, L_3).

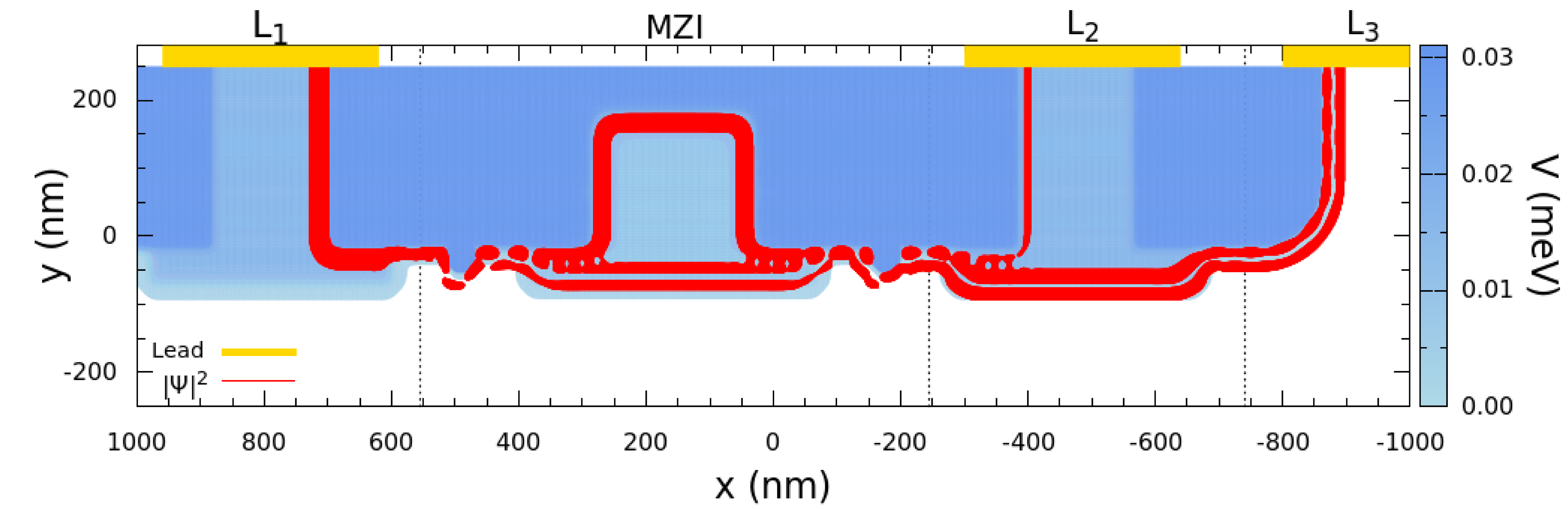

Acknowledgements

We acknowledge the CINECA award under the ISCRA initiative, for the availability of high performance computing resources and support (Iscra C projects 'MINTERES').

References

[1] A. Beggi et al. *J. Phys.: Cond. Matt.* **27**, 475301 (2015)

[2] V. Giovannetti et al. *Phys Rev B* **77**, 155320 (2008)

[3] P. Samuelsson et al. *Phys Rev Letters* **92**, 026805 (2004)